Adsorption (2013) 19:1019–1025
DOI 10.1007/s10450-013-9510-y

EXAFS and DFT studies of microscopic structure with different density upon Zn(II) adsorption on anatase TiO_2

Yuhuan Yang · Hao Chen · Changqing Ye

Received: 26 March 2010 / Accepted: 14 September 2012 / Published online: 23 February 2013

Abstract Microscopic structures of Zn(II) adsorbed on anatase TiO_2 surface with different densities were studied using extended X-ray absorption fine structure (EXAFS) spectroscopy and density functional theory (DFT) calculation. Quantitative analysis of the EXAFS spectra showed that microscopic structures of Zn(II) were fourfold coordinated complexes, and different microscopic structures were present of the solid surface. Three modes of corner–corner/sharing-corner/sharing-edge adsorptions on anatase (101) face cluster were calculated by the DFT method. The results from DFT method were consistent with the EXAFS fittings. The optimized Zn–O average distance of the Zn–O tetrahedron was determined as about 2.00 Å. The Zn–Ti distance was 3.69 Å for the corner–corner adsorption, 3.35 Å for the sharing-corner adsorption, and 3.02 Å for the sharing-edge adsorption. According to the adsorption energies calculated by the DFT method, the microscopic structure of corner–corner adsorption was less stable than those of the other adsorption modes. With the increasing adsorption density, the corner–corner adsorption mode would be enhanced more intensively than the other adsorption modes.

Keywords Zn · Anatase TiO_2 · Adsorption density · Adsorption microscopic structure · EXAFS · DFT

Y. Yang (✉) · C. Ye
School of Public Health, Nantong University, Nantong 226019, Jiangsu Province, People's Republic of China
e-mail: yangyuhuan77@yahoo.com.cn

Y. Yang · H. Chen
State Key Laboratory of Environmental Aquatic Chemistry, Research Center for Eco-Environmental Sciences, Chinese Academy of Sciences, Beijing 100085, People's Republic of China

1 Introduction

Adsorptions at the solid–water interface play a major role in controlling the fate and transport of heavy metals in natural aquatic environments. Understanding the binding mechanism of these metals to sediment surfaces was vital to accurately assess the hazards and risks of contaminated sediments in aquatic systems (Muller and Sigg 1990; Scheidigger et al. 1997). Macroscopic experiments provide information on bulk equilibrium and kinetic processes, and numerous macroscopic studies have laid down a solid theoretical basis for understanding the metal ion sorption mechanisms; however, to determine the molecular mechanisms, novel techniques such as X-ray absorption spectroscopy (XAS) and quantum calculation is needed.

EXAFS spectroscopy is uniquely suited to determine the average coordination environment. Importantly, samples can approach conditions found in the environment, the element of interest can be presented at concentrations as low as 0.05 wt% (depending on experimental conditions), and because no vacuum is required, the samples can contain water and be at room temperature (Brown et al. 1995; Charlet and Manceau 1993). These factors have been exploited by numerous workers since EXAFS spectroscopy became available (Zhang et al. 2001; Papelis et al. 1995; Roe et al. 1991; Waychunas et al. 1993, 1995). In recent years, the technique has been increasingly employed for providing structural and compositional information of surface complexes (Trainor et al. 2000; Trivedi et al. 2001), which often offers critical insights into the underlying adsorption–desorption mechanisms (Nachtegaal and Sparks 2004; Lee et al. 2004; Ragnarsdottir and Collins 1999). Current EXAFS methods can only determine the averaged microstructures. These averaged results can't help us to understand the adsorption system real structure and the core metal ions' stoichiometry. Basing on visual mode,

quantum chemical calculations are therefore an important tool for understanding the mechanisms of environmentally relevant chemical processes.

The aim of this study was to clarify the microscopic structure with the different adsorption density basing of Zn(II) adsorption on anatase TiO_2 with macrojar experiments and novel techniques. The extended EXAFS spectroscopy was employed to monitor the possible microscopic structure of the adsorption system, and Ab initio quantum mechanical modeling was used to complement and assist EXAFS data interpretation for samples of metal ions adsorbed on oxide-mineral. The results provide an enhanced molecular scale description of the fundamental processes leading to adsorption. This new information should lead to an improved understanding of Zn mobility and attenuation in the environment and allow quantitative modeling of these processes.

We chose to study Zn(II) adsorption on TiO_2 for several reasons. First, The sorption of dissolved Zn onto hydrous metal oxides, clays, and organic matter has been observed to play an important role in controlling the dissolved Zn concentrations in soils and natural waters (Kiekens and Alloway 1990; Vymazal 1985; Brummer et al. 1983; Tessier et al. 1989; Coston et al. 1995). We have observed Zn configuration of hydration in solution with changing pH. Zn(II) is present in the form of octahedron in acidic solutions and tetrahedron in alkaline solutions (Zhu 2005; Li et al. 2003). Second, TiO_2 has been intensively studied as an adsorbent for heavy metals owing to its high chemical stability in acidic and alkaline solutions (Towle et al. 1999; Kim and Chung 2001; Barakat 2005). Third, the study of Zn(II) adsorption on TiO_2 has thus provided a much better understanding on the relative importance of the different types of surface site than would have been possible by simply varying surface loading on a single mineral. Lastly, adsorption samples' surface properties do not change over the timescales of EXAFS experiments (hours to days). The EXAFS signal–noise ratio in the Zn(II)–TiO_2 system is much higher than other Zn(II)–metal oxide systems (Li et al. 2008).This choice is more reliable for analysing the mechanism at atomic levels in summary, second last line calculated energy.

2 Materials and methods

2.1 Materials

Zn(II) stock solution of 100 mg/L was obtained by dissolving $Zn(NO_3)_2{\cdot}6H_2O$ with Milli-Q water, and was demarcated with standard Zn(II) solution purchased from National Research Center for Certified Reference Material (CRM).

Anatase type nano TiO_2 was used as the adsorbent in our experiments, which was obtained from the Beijing Century Science and Technology Co. Ltd. The points of zero charge (PZC) were found to be 6.3, The N_2-BET (Micromeritics Inc., USA) surface areas of anatase were measured to be 200 ± 2 m^2/g, and the XRD (Rigaku, D/MAX-RC, Japan) patterns revealed that the TiO_2 was pure anatase-type TiO_2. TEM (H-7,500, Hitachi, Japan) analysis showed that the TiO_2 powder was in uniform particle size in water solution and their average diameter turned out to be 0.88 μm.

2.2 Batch sorption experiment

Sorption experiments were carried out with 1 g/L TiO_2, ionic strength solutions 0.1 mol/L KNO_3 at T = 5 °C. The pH values were controlled at 6.3 according to the pH edge experiment. An equilibrium period of 24 h was applied in the batch experiments.

2.3 EXAFS analysis

EXAFS data were collected at the BL-12C XAFS experimental station of the photon factory (PF) of the KEK in Japan. All adsorption samples were recorded using a 19-element SSD at the K-edge(9,659 eV) of Zn in the fluorescence mode. The reference compounds of ZnO(s) powders and Zn(II) solutions were recorded in the transmission mode.

EXAFS data analysis was performed using the WinXAS3.1 following the standard procedures (Ressler 1998), background absorbance of the spectra was removed, and EXAFS (chi) data were plotted as a function of electron wavenumber k (inverse Å). The extracted EXAFS function was weighted by k3 to enhance the radial structure function (RSF). Single and multishell in the RSF were isolated and back-transformed (the Fourier-backtransformed and processed with window widths of R-interval was 0.8–2.1 Å for the first shell and 2.35–3.75 Å for the second shell), and then the filtered data were converted into an amplitude (envelope) function and a phase function. The amplitude reduction factor (S_0^2) was fixed at 0.87 for data fitting accounting for this data relating to the measuring instrument. Using a nonlinear least squares fit procedure with a theoretical reference model compound was generated by FEFF8 (Ankudinov et al. 1998) with Webatom (Ravel 2001). EXAFS fittings were carried out by systematically refining the bond lengths R, Debye–Waller factors, σ^2, and inner potential corrections ΔE_0, for the models considered. The edge shifts (E_0) for all shells were constrained to be equal.

2.4 Calculation method

Quantum mechanical calculations of cluster geometries and energies were done using the Gaussian 03 code (Frich et al. 2004) which implements density functional theory for

finite clusters and molecules using the linear combination of atomic orbital formalism.6–31 G basis set was employed to O–H atoms, Lanl2dz basis set and pseudo-potentials were employed to Ti Zn atoms.

The TiO_2(101) crystal face was thermodynamically stable surface, and this surface constitutes >94 % of TiO_2 crystal face minerals (Ulrike 2003; Vittadini et al. 2000). In this work, two Ti atom octahedron adsorption clusters were employed to represent the TiO_2(101) crystal face as in Fig. 1. In order to avoid boundary effect and decrease the whole cluster charge, it was needed to add hydrogen on the oxygen dangling bond. In the process of optimization, only the atoms which were bound to Zn atoms were optimized on the adsorption cluster, and other atoms were fixed to keep the TiO_2 cluster as a bulk structure. The surface optimization can avoid severe deviation from the actual structure as the adsorption cluster is comparatively small (Ladeira et al. 2001).

3 Results and discussion

3.1 Macroscopic assessment of Zn(II) sorption on TiO_2

Fig. 2 showed the adsorption isotherm of the adsorption Density increasing with the Zn(II) ion equilibrium concentration in solution *n* the jar experiment after 24 h adsorption equilibrium.

In order to confirm the microscopic structure of different densities, we selected two samples, i.e., S1 and S2 as shown in Fig. 2 as the EXAFS testing points.

3.2 EXAFS analysis

The EXAFS spectra with fitting of Zn(II) sorbed on anatase TiO_2 under two adsorption densities are shown in Fig. 3. Spectra for ZnO and the aqueous $Zn(NO_3)_2$(i.e. hydrous Zn(II)) solution are also included for comparison. The top two spectra in Fig. 3 are ZnO and the aqueous $Zn(NO_3)_2$,

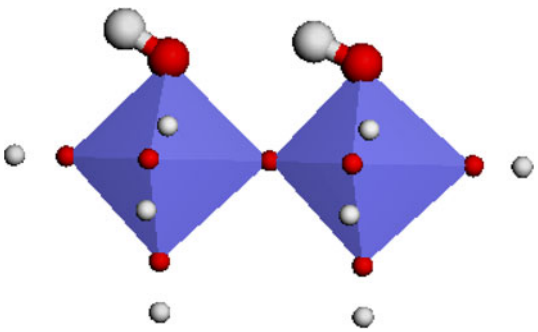

Fig. 1 $Ti_2O_9H_{11}$ cluster of anatase TiO_2(101) surface (*white ball*: H atom; *red ball*: O atom; *purple ball*: Ti atom) (Color figure online)

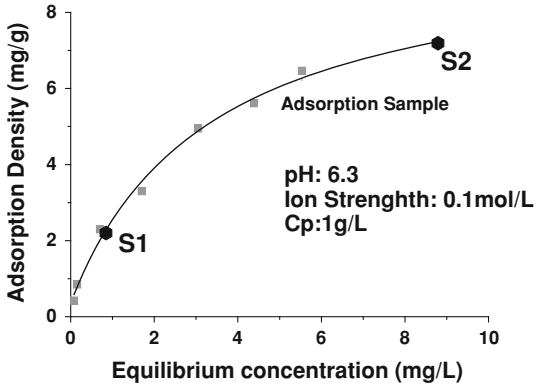

Fig. 2 Adsorption isotherm of Zn(II) adsorption on anatase TiO_2 (Cp = 1 g/L, S1, S2 are the sampling points for EXAFS analysis)

and The others are the EXAFS spectra of lower and higher adsorption density on the Zn–TiO_2 adsorption isotherm from experiments (S1 and S2). Correspondingly, the theoretical best fits for all of these samples are also presented in Fig. 3, and the fitting results of the distance between the core atom and neighbor atom were listed in Table 1.

As shown from Table 1, the average Zn–O bond length is 2.08 Å and the coordination number is 5.8 for the reference Zn(II), compared with 1.97 Å and 4.32 for ZnO(s), respectively. This result agrees with previous work (Pan et al. 2004; Li et al. 2004; Bochatay and Persson 2000) that Zn(II) was sixfold coordinated with oxygen, and ZnO(s) was fourfold coordinated. As for the first shell of S1 and S2, the average Zn–O bond length, denoted as R in Table 1, is 2.00 and 1.98 Å, the coordination number is 4.52 and 4.54 for S1 and S2 respectively. According to the literature, reporting that the most common coordination geometries of hydrous Zn(II) are octahedron with a Zn–O bond length of 2.07–2.18 Å and tetrahedron with a Zn–O bond length of 1.92–1.99 Å (Shock and Koretsky 1993; Spadini et al.

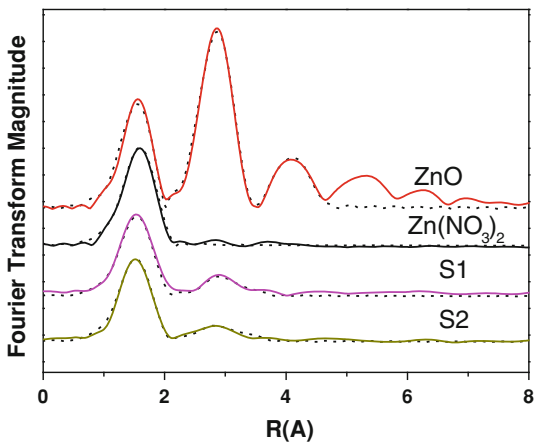

Fig. 3 Filtered EXAFS spectra (*lines*) and nonlinear least-squares fit (*dots*) of Samples S1 and S2 (S: Samples selected of Zn(II) adsorption on anatase TiO2 adsorption isotherm)

Table 1 EXAFS results for adsorbed Zn(II) on anatase TiO_2

Sample	The first Zn–O shell		The second Zn–Ti shell			
	CN	R (Å)	CN1	R1 (Å)	CN2	R2 (Å)
$Zn(NO_3)_2$	5.80	2.08	–	–	–	–
ZnO	4.32	1.97	–	–	–	–
S1	4.52	2.00	1.17	3.71	0.85	3.32
S2	4.54	1.98	1.95	3.71	1.13	3.28

CN coordination number, *CN1* single corner adsorption mode, *N2* double corner or single edge adsorption mode

1994), it could be argued that the sixfold coordination ($Zn(H2O)_2^{6+}$) changed to fourfold coordination because release of two H_2O (Spadini et al. 1994). Therefore, Zn(II) adsorbed on the TiO_2 surface herein is in fourfold tetrahedral coordination and it is transformed from the sixfold coordination ($Zn(H_2O)_2^{6+}$) by losing two H_2O molecules.

EXAFS analysis also provided information about the distance and coordination number (CN) of the second shell of Zn(II) ions and neighboring Ti atom. There are two kinds of distances, R_1 and R_2. R_1 was 3.71 Å, and R_2 was 3.32 Å and 3.28 Å for S1 and S2 respectively. Based on the literature that edge-sharing linkage, corner-sharing linkage (including double-corner and single-corner etc.) are the most common modes of binding between the polyhedron of hydrated metal ions and the octahedral of metal oxides (Pan et al. 2004; Li et al. 2004; Spadini et al. 1994), the varying R_2 accounted for the average change in distance of Zn–Ti with at least two microscopic adsorption modes, corresponding to different macroscopic adsorption Density.

3.3 DFT calculation

3.3.1 Geometry configuration

Based on the EXAFS results and polyhedral approach (Spadini et al. 1994; Combes et al. 1989) which was used for inferring the bonding mode of metal hydrated ions and oxide octahedron, three adsorption modes for the Zn(II) on anatase TiO_2 surface were accounted for as shown in Fig. 4.

According to DFT calculation, three optimized geometries corresponding to the Zn adsorbing on TiO_2(101), i.e. double corner (DC), single corner (SC) and single edge (SE) could be calculated, as shown in Fig. 5.

3.3.1.1 The first Zn–O shell According to the three different optimized geometries of Zn–TiO2 adsorption cluster, the distance of Zn–O for the first Zn–O shell could be divided into two groups. One group is the Zn–OH distance 1.95–1.97 Å, and the other group is the Zn–OH_2 distance 2.03–2.09 Å (Table 2). The average distance for the Zn–O shell is around 2.00 Å, which is consistent with the EXAFS results. The hydrated Zn(II) ions in water was six coordination at pH lower than 7 by EXAFS measurement (Zhu 2005; Li et al. 2003). The average distance for the Zn–O of hydrated Zn(II) ions is 2.12 Å by DFT calculation.

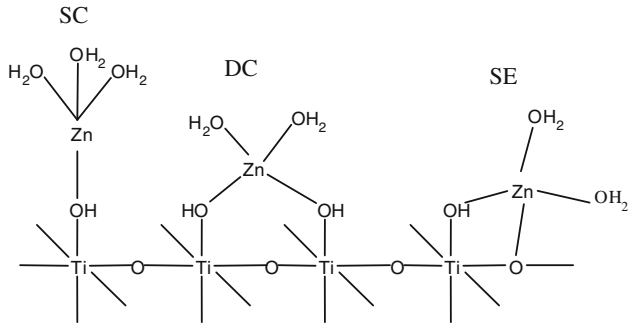

Fig. 4 The scheme of different adsorption modes of Zn(II) on anatase TiO_2 surface

3.3.1.2 The second Zn–Ti shell Table 2 showed three different Zn–Ti distances for the second Zn–Ti shell for the three different optimized geometries of Zn–TiO_2 adsorption cluster. The Zn–Ti distance is 3.68 Å for the SC adsorption mode, which is near to the distance of the second shell of Zn–Ti adsorption cluster by EXAFS fitting (3.71 Å). This proves that the adsorption cluster by EXAFS fitting has the SC adsorption mode. The distance of the Zn–Ti of the optimized geometries of Zn–TiO_2 adsorption cluster for DC and SE are 3.35 and 3.03 Å respectively. As shown in Table 2, the distance of 3.32 Å (or 3.28 Å) from the EXAFS fitting was close to the average distance of the DC and SE adsorption mode.

3.3.2 Adsorption energy

In order to compare the stability of these three adsorption geometries, we calculated the adsorption energy according the equation below:

$$E_{ads} = E_{adsorbate-substrate} - (E_{adsorbate} + E_{substrate})$$

The data in Table 3 showed different adsorption energy depending on adsorption geometries. The absolute energy

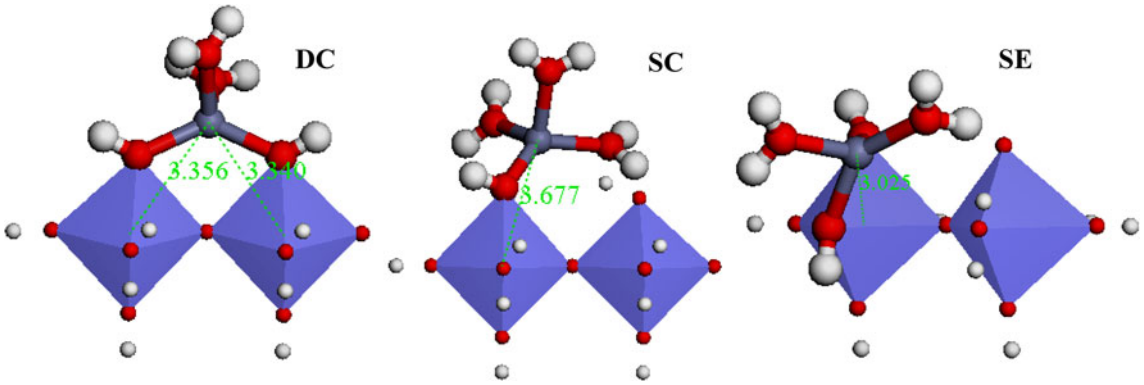

Fig. 5 Geometry structures of optimized adsorption structure (*white ball*: H atom; *red ball*: O atom; *purple ball*: Ti atom) (Color figure online)

Table 2 Calculated optimal geometries results of different adsorption modes

	d_{Zn-O} (Å)					d_{Zn-Ti} (Å)	
	Zn–OH		$Zn–OH_2$		Average	Zn–Ti	
DC	2.09	2.07	1.96	1.95	2.02	3.34	3.36
SE	2.05	2.05	1.97	1.96	2.01	3.03	
SC	2.06	2.03	2.05	1.96	2.02	3.68	
$Zn(H_2O)_6^{2+}$	–				2.12	–	

Table 3 Adsorption energy of different adsorption geometries

Adsorption geometries	Energy (hartree)			ΔE (hartree)	ΔE (KJ/Mol)
	Initial cluster	$Zn(H_2O)_4$ cluster	Adsorption cluster		
DC	−952.201	−370.71	−1170.234	−0.094	−247.909
SE	−952.201	−370.71	−1169.924	−0.078	−204.789
SC	−952.201	−370.71	−1246.608	−0.083	−218.697

value of −247.909 kJ/mol for the DC cluster is the lowest among these three geometries. This explained why DC was the most stable geometry cluster. The sequence of the two other stable is SC and SE. The greater the absolute value of ΔE is, the easier the adsorption reaction occurs.

4 Summary

From the EXAFS result, there existed at least two types of distance for the second Zn–Ti shell of the Zn–TiO_2 adsorption cluster. By geometry optimized DFT calculation, there were three types Zn–Ti distance for the different adsorption geometry cluster. According to the reaction energy DFT calculation, SE adsorption cluster is the easiest reaction among these three adsorptions, the DC adsorption cluster is the most stable geometry configuration.

As the results showed that there were different microscopic structures between the lower adsortption Density and the higher adsorption on the Zn–TiO_2 isotherm. The coordination number of the first Zn–O shell remained the same as four coordination at both lower and higher adsortption Density. The second coordination number of the second Zn–Ti shell is 1.17 Å at the lower adsortption Density, and it changes to 1.95 Å with the increase of adsorption Density. Comparing the coordination number increased with the adsorption Density by the DFT optimized the geometry, the Zn–Ti distance keeps 3.71 Å, indicating one type of SC adsorption mode. The SC adsorption mode number increased with the Zn(II) ions adsorbed on TiO_2. The coordination number of 0.85 for the second Zn–Ti shell present at lower adsorption density, and this value changed to 1.13 Å with increasing adsorption Density. According to the calculated energy, the SE adsorption mode occurred more than the DC adsorption mode with increasing the adsorption density.

Acknowledgments The authors thank the institute of high energy physics Chinese academy of sciences for the EXAFS spectrum unscrambling and soft support, and thank the supercomputing center

of Chinese academy of sciences for the DFT soft. This work was financially supported by NNSF of China (Grant No. 21107054).

References

Ankudinov, A.L., Ravel, B., Rehr, J.J., Conradson, S.D.: Real-space multiple scattering calculation of XANES. Phys. Rev. B **58**, 7565–7576 (1998)

Barakat, M.A.: Adsorption behavior of copper and cyanide ions at TiO_2–solution interface. J. Colloid Interface Sci. **291**, 345–352 (2005)

Bochatay, L., Persson, P.: Metal ion coordination at the water–manganite (γ-MnOOH) interface: II. an EXAFS study of Zn(II). J. Colloid Interface Sci. **229**, 593–599 (2000)

Brown Jr, G.E., Parks, G.A., O'Day, P.A.: In: Pattrick, R.A.D., Vaughan, D.J. (eds.) Mineral Surfaces, pp. 129–183. Chapman and Hall, London (1995)

Brummer, G., Tiller, K.G., Herms, U., Clayton, P.M.: Adsorption–desorption and/or precipitation–dissolution processes of Zn in soils. Geoderma **31**, 337–354 (1983)

Charlet, L., Manceau, A.: Environmental analytical and physical chemistry series. In: Buffle, J., van Leeuwen, H.P. (eds.) Environmental Particles, vol. 2, pp. 117–164. Lewis Publishers, Boca Raton (1993)

Combes, J.M., Manceau, A., Calas, G., Bottero, J.Y.: Formation of ferric oxides from aqueous solutions: a polyhedral approach by X-ray absorption spectroscdpy: I. hydrolysis and formation of ferric gels. Geochim. Cosmochim. Acta **53**, 583–594 (1989)

Coston, J.A., Fuller, C.C., Davis, J.A.: Pb2 + and Zn2 + adsorption by a natural Aluminum- and Iron-bearing surface coating on an aquifer sand. Geochim. Cosmochim. Acta **59**, 3535–3547 (1995)

Frich, M.J., Trucks, G.W., Schlegel, H.B., Scuseria, G.E., Robb, M.A., Cheeseman, J.R., Montgomery Jr, J.A., Vreven, T., Kudin, K.N., Burant, J.C., Millam, J.M., Iyengar, S.S., Tomasi, J., Barone, V., Mennucci, B., Cossi, M., Scalmani, G., Rega, N., Petersson, G.A., Nakatsuji, H., Hada, M., Ehara, M., Toyota, K., Fukuda, R., Hasegawa, J., Ishida, M., Nakajima, T., Honda, Y., Kitao, O., Nakai, H., Klene, M., Li, X., Knox, J.E., Hratchian, H.P., Cross, J.B., Bakken, V., Adamo, C., Jaramillo, J., Gomperts, R., Stratmann, R.E., Yazyev, O., Austin, A.J., Cammi, R., Pomelli, C., Ochterski, J.W., Ayala, P.Y., Morokuma, K., Voth, G.A., Salvador, P., Dannenberg, J.J., Zakrzewski, V.G., Dapprich, S., Daniels, A.D., Strain, M.C., Farkas, O., Malick, D.K., Rabuck, A.D., Raghavachari, K., Foresman, J.B., Ortiz, J.V., Cm, Q., Baboul, A.G., Clifford, S., Cioslowski, J., Stefanov, B.B., Liu, G., Liashenko, A., Piskorz, P., Komaromi, I., Martin, R.L., Fox, D.J., Keith, T., Al-Laham, M.A., Peng, C.Y., Nanayakkara, A., Challa-combe, M., Gill, P.M.W., Johnson, B., Chen, W., Wong, M.W., Gonzalez, C., Pople, J.A.: Gaussian 03, Revision C.02. Gaussian, Wallingford (2004)

Kiekens, L.: In: Alloway, B.J. (ed.) Heavy Metals in Soils, p. 284. Blackie, London (1990)

Kim, M.S., Chung, J.G.: A study on the adsorption characteristics of orthophosphates on rutile-type titanium dioxide in aqueous solutions. J. Colloid Interface Sci. **233**, 31–37 (2001)

Ladeira, A.C.Q., Ciminell, V.S.T., Duarte, H.A., Alves, M.C.M., Ramos, A.Y.: Mechanism of anion retention from EXAFS and density functional calculations: arsenic (V) adsorbed on gibbsite. Geochim. Cosmochim. Acta **65**, 1211–1217 (2001)

Lee, S., Anderson, P.R., Bunker, G.B., Karanfil, C.: EXAFS study of Zn sorption mechanisms on montmorillonite. Environ. Sci. Technol. **385**, 426–5432 (2004)

Li, X., Pan, G., Qin, Y., Hu, T., Xie, Y., Chen, H.: EXAFS studies on adsorption microscopic structures of Zn at manganite-water interface. J. High Energy Phys. Nucl. Phys. **27**, 23–27 (2003). Chinese edition

Li, X., Pan, G., Qin, Y., Hu, T., Wu, Z., Xie, Y.: EXAFS studies on adsorption–desorption reversibility at manganese oxide–water interfaces: II. reversible adsorption of Zn on δ-MnO_2. J. Colloid Interface Sci. **271**, 35–40 (2004)

Li, W., Pan, G., Zhang, M.Y., Zhao, D.Y., Yang, Y.H., Chen, H., He, G.Z.: EXAFS studies on adsorption irreversibility of Zn(II) on TiO_2: temperature dependence. J. Colloid Interface Sci. **319**, 385–391 (2008)

Muller, B., Sigg, L.: Interaction of trace metals with natural particle surfaces: comparison between adsorption experiments and field measurements. Aquat. Sci. **52**, 75–92 (1990)

Nachtegaal, M., Sparks, D.L.: Effect of iron oxide coatings on zinc sorption mechanisms at the clay-mineral/water interface. J. Colloid Interface Sci. **276**, 13–23 (2004)

Pan, G., Qin, Y., Li, X., Hu, T., Wu, Z., Xie, Y.: EXAFS studies on adsorption–desorption reversibility at manganese oxides–water interfaces: I. irreversible adsorption of Zn onto manganite (γ-MnOOH). J. Colloid Interface Sci. **271**, 28–34 (2004)

Papelis, C., Brown Jr, G.E., Parks, G.A., Leckie, J.O.: X-ray absorption spectroscopic studies of cadmium and selenite adsorption on aluminum oxides. Langmuir **11**, 2041–2048 (1995)

Ragnarsdottir, K.V., Collins, C.R.: The mechanism of cadmium surface complexation on iron oxyhydroxide minerals. Geochim. Cosmochim. Acta **63**, 2971–2987 (1999)

Ravel, B.: ATOMS, crystallography for the X-ray absorption spectroscopist. J. Synchroton Radiat. **8**, 314–316 (2001)

Ressler, T.: WinXAS, a program for X-ray absorption spectroscopy data analysis under MS-windows. J. Synchrotron Radiat. **5**, 118–122 (1998)

Roe, A.L., Hayes, K.F., Chisholm-Brause, C.J., Brown Jr, G.E., Parks, G.A., Hodgson, K.O., Leckie, J.O.: In-situ X-ray absorption study of lead ion surface complexes at the goethite-water interface. Langmuir **7**, 367–373 (1991)

Scheidigger, A.M., Lamble, G.M., Sparks, D.L.: Spectroscopic evidence for the formation of mixed-cation hydroxide phases upon metal sorption on clays and Aluminum Oxides. J. Colloid Interface Sci. **186**, 118–128 (1997)

Shock, E.L., Koretsky, C.M.: Etal-organic complexes in geochemical processes: calculation of standard partial molal thermodynamic properties of aqueous acetate complexes at high pressures and temperatures. Geochim. Cosmochim. Acta **57**, 4899–4922 (1993)

Spadini, L., Manceau, A., Schindler, P.W., Charlet, L.: Structure and stability of Cd^{2+} surface complexes on ferric oxides: 1. Results from EXAFS spectroscopy. J. Colloid Interface Sci. **168**, 73–86 (1994)

Tessier, A., Carignan, R., Dubruel, B., Rapin, F.: Partitioning of Zn between the water column and the oxic sediments in lakes. Geochim. Cosmochim. Acta **53**, 1511–1522 (1989)

Towle, S.N., Brown, G.E., Parks, G.A.: Sorption of Co(II) on metal oxide surfaces: I. Identification of specific binding sites of Co(II) on (110) and (001) surfaces of TiO_2 (rutile) by Grazing-incidence XAFS spectroscopy. J. Colloid Interface Sci. **217**, 299–311 (1999)

Trainor, T.P., Brown, G.E., Parks, G.A.: Adsorption and precipitation of aqueous Zn(II) on alumina powders. J. Colloid Interface Sci. **231**, 359–372 (2000)

Trivedi, P., Axe, L., Tyson, T.A.: An analysis of Zn sorption to amorphous versus crystalline iron oxides using XAS. J. Colloid Interface Sci. **244**, 230–238 (2001)

Ulrike, D.: The surface science of TiO_2. Surf. Sci. Rep. **48**, 53–229 (2003)

Vittadini, A., Selloni, A., Rotzinger, F.P., Gratzel, M.: Structure and energetics of water adsorbed at TiO_2 anatase (101) and (001) surfaces. J. Phys. Chem. C **104**, 1300–1306 (2000)

Vymazal, J.: Occurrence and chemistry of Zn in freshwaters—its toxicity and bioaccumulation with respect to algae: a review. Part 1: occurrence and chemistry of Zn. Acta Hydrochem. Hydrobiol. **13**, 627–654 (1985)

Waychunas, G.A., Rea, B.A., Fuller, C.C., Davis, J.A.: Surface chemistry of ferrihydrite:Part 1.EXAFS study of geometry of coprecipitated and adsorbed arsenate. Geochim. Cosmochim. Acta **57**, 2251–2269 (1993)

Waychunas, G.A., Davis, J.A., Fuller, C.C.: Geometry of sorbed arsenate on ferrihydrite and crystalline FeOOH. Geochim. Cosmochim. Acta **59**, 3655–3661 (1995)

Zhang, P.C., Brady, P.V., Arthur, S.E., Zhou, W.Q.: Adsorption of barium (II) on montmorillonite: an EXAFS study. Colloids Surf. A **190**, 239–249 (2001)

Zhu, M., Pan, G.: Quantum chemical studies of mononuclear zinc species of hydration and hydrolysis. J. Phys. Chem. A **109**, 7648–7652 (2005)